Weakly-supervised segmentation of referring expressions

Robin Strudel, Ivan Laptev, Cordelia Schmid

Weakly-supervised segmentation of referring expressions

Robin Strudel, Ivan Laptev, and Cordelia Schmid

Inria, Ecole normale supérieure, CNRS,
PSL Research University, 75005 Paris, France.

Abstract. Visual grounding localizes regions (boxes or segments) in the image corresponding to given referring expressions. In this work we address image segmentation from referring expressions, a problem that has so far only been addressed in a fully-supervised setting. A fully-supervised setup, however, requires pixel-wise supervision and is hard to scale given the expense of manual annotation. We therefore introduce a new task of weakly-supervised image segmentation from referring expressions and propose Text grounded semantic SEGgmentation (TSEG) that learns segmentation masks directly from image-level referring expressions without pixel-level annotations. Our transformer-based method computes patch-text similarities and guides the classification objective during training with a new multi-label patch assignment mechanism. The resulting visual grounding model segments image regions corresponding to given natural language expressions. Our approach TSEG demonstrates promising results for weakly-supervised referring expression segmentation on the challenging PhraseCut and RefCOCO datasets. TSEG also shows competitive performance when evaluated in a zero-shot setting for semantic segmentation on Pascal VOC.

Keywords: Weakly-supervised learning, referring expression segmentation, visual grounding, vision and language.

1 Introduction

Image segmentation is a key component for a wide range of applications including virtual presence, virtual try on, movie post production and autonomous driving. Powered by modern neural networks and supervised learning, image segmentation has been significantly advanced by recent work [9,11,42,53]. While most of this work addresses semantic segmentation, the more general problem of visual grounding beyond segmentation of pre-defined object classes remains open. Moreover, the majority of existing method assume full supervision and require costly pixel-wise manual labeling of training images which prevents scalability.

Manual supervision has been recognized as a bottleneck in many vision tasks including object detection [5,30,37] and segmentation [2,3,18,68], text-image and text-video matching [44,47] and human action recognition [6,19]. To this end,

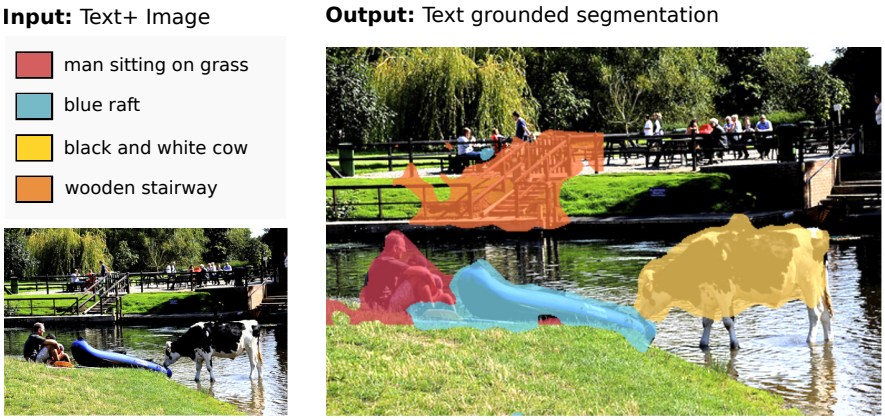

Fig. 1: Given an image and a set of referring expressions such as *man sitting on grass* and *wooden stairway*, TSEG segments the image regions corresponding to the input expressions. Here we show results of our approach TSEG for a test image of the PhraseCut dataset. Contrary to other existing methods, TSEG only uses image-level referring expressions during training and hence does not require pixel-wise supervision.

self-supervised methods explore regularities in images and videos and learn transferable visual representations without manual supervision [10,14]. Other weakly-supervised methods exploit partial and possibly noisy supervision that is either readily-available or less costly to annotate [5,44]. In particular, weakly-supervised methods for image segmentation avoid the costly pixel-wise annotation and limit supervision to image-level labels [2,3,18,68]. Such methods, however, remain restricted to predefined sets of classes.

A referring expression is a short text describing a visual entity such as *man sitting on grass* or *wooden stairway*, see Fig. 1. The task of referring expression segmentation [24,64] generalizes image segmentation from pre-defined object classes to free-form text. Given an input image and text queries (referring expressions), one should generate image segments for each referring expression. This enables segmentation using compositional referring expressions such as *man sitting on grass* and *wooden stairway*. Despite the promise of scalability, existing approaches to referring expression segmentation require pixel-wise annotation and, hence, remain limited by the size of existing datasets.

Our work aims to advance image segmentation beyond limitations imposed by the pre-defined sets of object classes and the costly pixel-wise manual annotations. Towards this goal, we propose and address the new task of *weakly-supervised referring expression segmentation*. As this task comprises difficulties of the weakly-supervised segmentation and referring expression segmentation, it introduces new challenges. In particular, existing weakly-supervised methods for image segmentation typically rely on the completeness of image-level labels, i.e., the absence of a car in the annotation implies its absence in the image. This

completeness assumption does not hold for referring expression segmentation. Furthermore, the vocabulary is open and compositional.

To address the above challenges and to learn segmentation from text-based image-level supervision, we introduce a new global weighted pooling mechanism denoted as Multi-label Patch Assignment (MPA). Our method for Text grounded semantic SEGgmentation (TSEG) incorporates MPA and extends the recent transformer-based Segmenter architecture [53] to referring expression segmentation. We validate our method and demonstrate its encouraging results for the task of weakly-supervised referring expression segmentation on the challenging PhraseCut [59] and RefCOCO [65] datasets. We also evaluate TSEG in a zero-shot setting for semantic segmentation and obtain competitive performance on the Pascal VOC dataset [16].

In summary, our work makes the following three contributions. (i) We introduce the new task of weakly-supervised referring expression segmentation and propose an evaluation based on the PhraseCut and RefCOCO datasets. (ii) We propose TSEG, a new method addressing weakly-supervised referring expression segmentation with a multi-label patch assignment score. (iii) We demonstrate advantages of TSEG through a number of ablations and experimental comparisons on the challenging PhraseCut and RefCOCO datasets. Furthermore, we demonstrate competitive results for zero shot semantic segmentation on PASCAL VOC.

2 Related Work

Weakly-supervised semantic segmentation. Given an image as input, the goal of semantic segmentation is to identify and localize classes present in the image, e.g. annotate each pixel of the input image with a class label. Weakly-supervised Semantic Segmentation (WSS) has been introduced by [68] and trains models using only image labels as supervision. Zhou *et al.* [68] use Class Activation Maps (CAMs) of a Fully Convolutional Network (FCN) combined with Global Average Pooling (GAP) to obtain segmentation maps with a pooling mechanism. As CAMs tend to focus on most discriminative object parts [57], recent methods deploy more elaborate multi-stage approaches using pixel affinity [1,2], saliency estimation [17,18,27,35,56,66] or seed and expand strategies [27,33,57].

While these methods provide improved segmentation, they require multiple standalone and often expensive networks such as saliency detectors [18,27,66] or segmentation networks based on pixel-level affinity [1,2]. Single-stage methods have been developed based on multiple instance learning (MIL) [46] or expectation-maximization (EM) [45] approaches where masks are inferred from intermediate predictions. Single-stage methods have been overlooked given their inferior accuracy until the work of Araslanov *et al.* [3] that proposed an efficient single-stage method addressing the limitations of CAMs. Araslanov *et al.* [3] introduces a global weighted pooling (GWP) mechanism which we extend in this work with a new multi-label patch assignment mechanism (MPA). In contrast to prior work on weakly-supervised semantic segmentation, TSEG is a single-stage

method that scales to the challenging task of referring expression segmentation.

Referring expression segmentation. Given an image and a referring expression, the goal of referring expression segmentation is to annotate the input image with a binary mask localizing the referring expression. A fully-supervised method [24] proposed to first combine features of a CNN with a LSTM and then decode them with a FCN. To improve segmentation masks, [64] uses a two-stage method based on Mask-RCNN [23] features combined with a LSTM. To overcome the limitation of FCN to model global context and learn richer cross-modal features, *state-of-the-art* approaches [13,25,63] use a decoding scheme based on cross-modal attention. Despite their effectiveness, these methods are fully-supervised which limits their scalability. Several weakly-supervised approaches tackle detection tasks such as referring expression comprehension [7,21,40,41,60] by enforcing visual consistency [7], learning language reconstruction [40] or with a contrastive-learning objective [21]. These methods rely on an off-the-shelf object detector, Faster-RCNN [49], to generate region proposals and are thus limited by the object detector accuracy. None of these weakly-supervised methods address the problem of referring expression segmentation which is the focus of our work. TSEG is a novel approach that tackles weakly-supervised referring expression segmentation based on the computation of patch-text similarities with a new multi-label patch assignment mechanism (MPA).

Transformers for vision and language. Transformers [55] are now state of the art in many natural language processing (NLP) [12] and computer vision [4,11,15,42,53] tasks. Such methods capture long-range dependencies among tokens (patches or words) with an attention mechanism and achieve impressive results in the context of vision-language pre-training at scale with methods such as CLIP [47], VisualBERT [38], DALL-E [48] or ALIGN [28]. Specific to referring expressions, MDETR [29] recently proposed a method for visual grounding based on a cross-modal transformer decoder trained on a fully-supervised visual grounding task. Several methods perform zero-shot semantic segmentation with pre-trained fully supervision models [20,62,67,69]. Most similar to our work, GroupViT [61] relies on a large dataset of 30M image-text pairs to learn segmentation masks from text supervision, but the objective function and model architecture are different.

Our TSEG approach aims to learn patch-text associations while using only image-level annotations with referring expression. TSEG builds on CLIP [47] and uses separate encoders for different modalities with a cross-modal late-interaction mechanism. Its segmentation module builds on Segmenter [53] which shows that interpolating patch features output by a Vision Transformer (ViT) [15] is a simple and effective way to perform semantic segmentation. Here, we extend this work to perform cross-modal segmentation. TSEG leverages a novel patch-text interaction mechanism to compute both image-text matching scores and pixel-level text-grounded segmentation maps in a single forward pass.

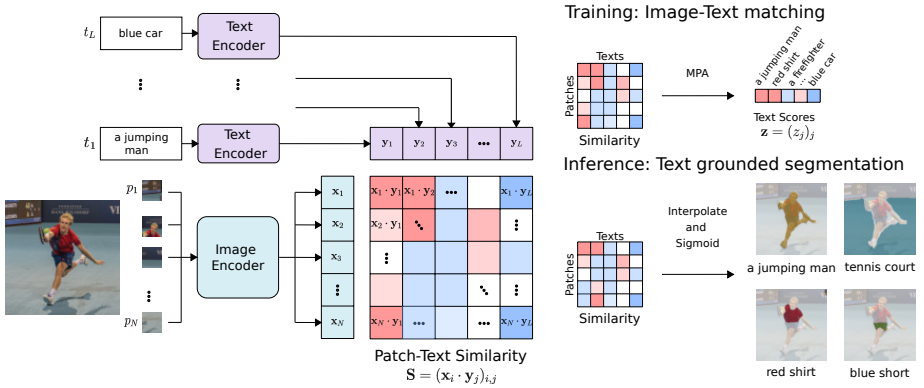

Fig. 2: Overview of our approach TSEG. (Left) Image patches and referring expressions are mapped with transformers to patch and text embeddings and then compared by computing patch-text cosine similarity scores. (Right - Training) Our global pooling mechanism with multi-label patch assignment (MPA) reduces patch-text similarity scores to image-level labels to train the model for referring expression classification. (Right - Inference) Sequences of patch scores (columns) are rearranged into 2D masks and bilinearly interpolated to obtain pixel-level referring expression masks.

3 Method

TSEG takes as input an image and a number of referring expressions and outputs a confidence score (Fig. 2, top-right) along with a segmentation mask (Fig. 2, bottom-right) for each referring expression. During training no segmentation masks are available and image-level labels are used to train referring expression segmentation (Fig. 2, top-right). TSEG is based on image patch-text matching (Fig. 2 left). An image encoder maps the input image to a sequence of patch tokens and a text encoder maps each input referring expression to a single text token. The tokens are then projected to a common embedding space and patch-text cosine similarities are computed as described in Section 3.1. To obtain an image-level score for each referring expression, the patch-text similarity matrix is summarized along the patch dimension. To do so, we introduce a novel multi-label patch assignment (MPA) mechanism described in Section 3.2. The model is then trained end-to-end to predict the corresponding image-text pairs as described in Section 3.3. At inference, the patch-text matrix is simply interpolated for patches to obtain pixel-level masks as described in Section 3.3. The choice of an appropriate global pooling mechanism is important to learn accurate segmentation maps as illustrated in Figure 3. We evaluate its impact in Section 4 and show that the novel multi-label patch assignment mechanism outperforms existing ones by a significant margin.

3.1 Patch-text similarity matrix

In this section we describe how to compute the similarity matrix between patches of an image and several referring expressions. We consider an image represented by N patches $p_1, ..., p_N$ and a set of L referring expressions $t_1, ..., t_L$. Patches are encoded by tokens $(\mathbf{x}_1, ..., \mathbf{x}_N)$, each referring expression consists of several words and is encoded by one token $(\mathbf{y}_1, ..., \mathbf{y}_L)$. The resulting similarity matrix is $\mathbf{S} = (\mathbf{x}_i \cdot \mathbf{y}_j)_{i,j} \in \mathbb{R}^{N \times L}$. See Figure 2 left.

Image encoder. An image $I \in \mathbb{R}^{H \times W \times C}$ is split into a sequence of patches of size (P, P). Each image patch is then linearly projected and a position embedding is added to produce a sequence of patch tokens $(p_1, ..., p_N) \in \mathbb{R}^{N \times D_I}$ where $N = HW/P^2$ is the number of patches, D_I is the number of features. A transformer encoder maps the input sequence to a sequence of contextualized patch tokens $(\mathbf{x}_1, ..., \mathbf{x}_N) \in \mathbb{R}^{N \times D_I}$. See more details in Section 4.2.
Text encoder. For each referring expression t_j, which can consist of multiple words, we extract one token $\mathbf{y}_j$. To do so the text t_j is tokenized into words using lower-case byte pair encoding (BPE) [51] and [BOS], [EOS] tokens are added to the beginning and the end of the sequence. A sequence of position embedding is added and a transformer encoder maps the input sequence to a sequence of contextualized word tokens from which the [BOS] token is extracted to serve as a global text representation $\mathbf{y}_j \in \mathbb{R}^{D_T}$.
Patch-text similarity scores. The visual and textual tokens are linearly projected to a multi-modal common embedding space and L^2-normalized. From the patch tokens $(\mathbf{x}_1, ..., \mathbf{x}_N)$ and the global text tokens $(\mathbf{y}_1, ..., \mathbf{y}_L)$, we compute patch-text cosine similarities as the scalar product and obtain the similarity matrix

$$\mathbf{S} = (s_{i,j})_{i,j} = (\mathbf{x}_i \cdot \mathbf{y}_j)_{i,j}, \tag{1}$$

with $\mathbf{S} \in \mathbb{R}^{N \times L}$. The similarities are in the range $[-1, 1]$ and scaled with a learnable temperature parameter $\tau > 0$ controlling their range.

3.2 Global Pooling Mechanisms

To leverage image-level text supervision, we need to map the matrix $\mathbf{S} \in \mathbb{R}^{N \times L}$ of patch-text similarities to an image-level score for each referring expression, i.e., $\mathbf{z} \in \mathbb{R}^L$. The score vector $\mathbf{z}$ allows us to compute a classification loss using ground truth referring expressions. Note that we cannot compute per-pixel losses given the lack of pixel-wise supervision in weakly-supervised settings.

Global average and max pooling (GAP-GMP). A straightforward way of pooling is global average pooling (GAP), where we average the similarities for a given referring expression over all patches of an image:

$$z_j^{GAP} = \frac{1}{N} \sum_{i=1}^{N} s_{i,j}. \tag{2}$$

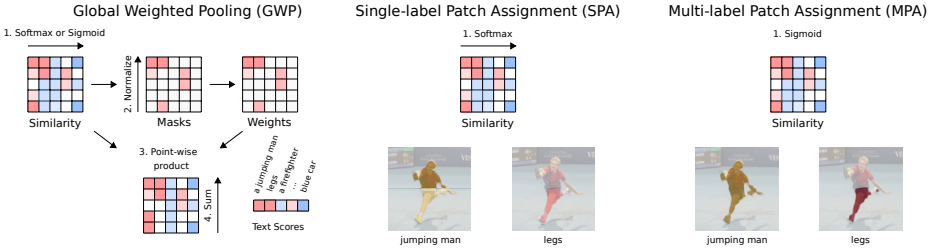

Fig. 3: (Left) A patch assignment mechanism computes masks from patch-text similarities, the masks are used as weights in the global weighed pooling. (Center) SPA: assignment with a softmax on text channels, softly enforcing a single label per patch. (Right) MPA: assignment with a sigmoid, generalizing to multiple labels per patch.

This score is expected to be high if the referring expression is contained in the image. However, the score is dependent on the object size and results in low scores for small objects. An alternative to GAP is global max pooling (GMP):

$$z_j^{GMP} = \max_i(s_{i,j}). \tag{3}$$

The max operation in GMP decreases the influence of the object size, however it tends to focus on most discriminative regions of a class [57].

Global weighted pooling (GWP). To address the shortcomings of GAP and GMP, we follow [3] and make use of weighted pooling. Global weighted pooling replaces the constant patch weights $1/N$ in the sum of GAP by weights $\mathbf{W} = (w_{i,j})_{i,j} \in \mathbb{R}^{N \times L}$. The final score of a referring expression is then the weighted average of similarities:

$$z_j^{GWP} = \sum_{i=1}^{N} w_{i,j} s_{i,j}, \tag{4}$$

as illustrated in Figure 3 left. In practice, $\mathbf{W}$ is defined in terms of spatially normalized mask scores $\mathbf{M} = (m_{i,j})_{i,j} \in \mathbb{R}^{N \times L}$, based on $w_{i,j} = m_{i,j}/(\sum_i m_{i,j} + \varepsilon)$ where $\varepsilon > 0$ allows for $\sum_i w_{i,j} = 0$ when mask scores are below a threshold. GAP is a particular case of GWP where $m_{i,j} = 1$ for all i, j and $\varepsilon = 0$. We next describe two methods to compute masks $\mathbf{M}$ from the similarity matrix $\mathbf{S}$.

Masks by single-label patch assignment (SPA) [3]. We aim at assigning patches to the relevant referring expression. To do so, we apply a softmax operation over all referring expressions $(\mathbf{y}_1, ..., \mathbf{y}_L)$ for each patch $\mathbf{x}_i$:

$$m_{i,j}^{SPA} = \frac{e^{s_{i,j}}}{e^{s_{bg}} + \sum_{j=1}^{L} e^{s_{i,j}}}. \tag{5}$$

We add a background column $(s_{i,0})_i$ and assign it a constant equal to $s_{bg} = 0$ for all patches $\mathbf{x}_i$. This allows to assign patches with low scores $s_{i,j} < 0$ to the

background. The masks are then soft assignments with $\sum_{j=0}^{L} m_{i,j} = 1$ for any patch i. This patch assignment can be viewed as multi-class classification which is typical for semantic segmentation where one pixel is matched to a *single label* as proposed by [3].

This single-label patch assignment (SPA) is illustrated in Figure 3 center. The softmax operation over referring expressions softly enforces the correspondence of a patch to one expression. However, this definition is problematic for referring expression segmentation where the masks of several expressions can overlap. We illustrate this in Figure 3 center where pixels corresponding to *jumping man* and *legs* have lower mask weights on the overlapping region. Such lower mask weights result in decreased image-level scores for both of the expressions.

Masks by multi-label patch assignment (MPA). We propose multi-label patch assignment (MPA) that overcomes the above limitations of SPA. For each patch $\mathbf{x}_i$, we rely on binary classification between a referring expression $\mathbf{y}_j$ and the background based on:

$$m_{i,j}^{MPA} = \frac{e^{s_{i,j}}}{e^{s_{bg}} + e^{s_{i,j}}}. \tag{6}$$

In this case, each patch can be assigned to multiple referring expressions, see Figure 3 right. The masks are not mutually exclusive and each referring expression can be assigned a score $m_{i,j}^{MPA} \in [0, 1]$ without softmax imposed constraints. Patch assignment is viewed as a multi-label classification problem, this property is highly beneficial when performing weakly-supervised referring expression segmentation, as shown in Section 4.

Image-text scores. We compute GWP scores $\mathbf{z}^{GWP}$ with (4) using the masks $\mathbf{M}$ defined according to one of the assignment mechanism defined in (5),(6). Then, we compute mask size scores $\mathbf{z}^{size}$ as

$$z_j^{size} = (1 - \overline{m}_j)^p \log(\lambda + \overline{m_j}), \tag{7}$$

with $\overline{m_j} = \frac{1}{N} \sum_{i=1}^{N} m_{i,j}$. This $\mathbf{z}^{size}$ is a size-penalty term introduced by [3] to enforce mask completeness, e.g. $z_j^{size} < 0$ for small masks. The magnitude of this penalty is controlled by λ. Due to the normalization, $\mathbf{W}$ used in GWP is invariant to the masks size $\mathbf{M}$ and $\mathbf{z}^{size}$ enforces masks to be complete. The final score defining the presence of a referring expression t_j in the image is defined as the sum:

$$z_j = z_j^{GWP} + z_j^{size}. \tag{8}$$

3.3 Training and inference

In the following we describe our weakly supervised and fully supervised training procedure. Furthermore, we present the approach used for inference.

Weakly-supervised learning. Weakly-supervised segmentation is usually addressed on datasets with a fixed number of classes. To handle the more general

case where visual entities in the image are defined by referring expressions we use referring expressions of samples in a mini-batch as positive and negative examples. Given a mini-batch containing (image, referring expression) pairs, the model has to predict the subset of referring expressions present in each image. For each image, we extract image-text scores $\mathbf{z} \in \mathbb{R}^L$ from the similarity matrix $\mathbf{S}$ using one of the pooling mechanism described in the previous section. Finally, we optimize over the scores to match ground truth pairings $\bar{\mathbf{z}}$ with the multi-label soft-margin loss function [2,3,58] as a classification loss,

$$\mathcal{L}_{cls}(\mathbf{z}, \bar{\mathbf{z}}) = \sum_{j=1}^{L} -\bar{z}_j \log\left(\sigma(z_j)\right) - (1 - \bar{z}_j) \log\left(\sigma(-z_j)\right),$$

where $\sigma(x) = 1/(1 + \exp(-x))$ is the sigmoid function. The loss encourages $z_j > 0$ for positive image-text pairs and $z_j < 0$ for negative pairs.

Fully-supervised learning. In the fully-supervised case, segmentation is learned from a dataset of images annotated with referring expressions and their corresponding segmentation masks. Only positive referring expressions $(\mathbf{y}_1, ..., \mathbf{y}_L)$ are passed to the text encoder and the similarity matrix $\mathbf{S}$ is bilinearly interpolated to obtain pixel-level similarities of shape $\mathbb{R}^{H \times W \times L}$. Then, we minimize the Dice loss between the sigmoid of the pixel-level similarities $\mathbf{M} = \sigma(\mathbf{S})$ and the ground truth masks $\overline{\mathbf{M}}$:

$$\mathcal{L}_{dice}(\mathbf{M}, \overline{\mathbf{M}}) = 1 - 2\frac{|\mathbf{M} \cap \overline{\mathbf{M}}|}{|\mathbf{M}| + |\overline{\mathbf{M}}|}, \tag{9}$$

where $|\mathbf{M}| = \sum_{i,j} m_{i,j}$ and $\mathbf{M} \cap \overline{\mathbf{M}} = (m_{i,j}\overline{m}_{i,j})_{i,j}$.

Inference. To produce segmentation masks, we reshape the patch-text masks $\mathbf{M} \in \mathbb{R}^{N \times L}$ into a 2D map and bilinearly interpolate it to the original image size to obtain pixel-level masks of shape $\mathbb{R}^{H \times W \times L}$. For SPA, pixel annotations are obtained by adding a background mask to $\mathbf{M}$ and applying an argmax over the refering expressions. For MPA, we threshold the values of $\mathbf{M}$ using the background score. For GAP and GMP, we follow the standard approach from [2] to compute the masks $\mathbf{M}$. Directly interpolating patch-level similarity scores to generate segmentation maps has been proven effective by Segmenter [53] in the context of semantic segmentation. Our decoding scheme is an extension of Segmenter linear decoding where the set of fixed class embeddings is replaced by text embeddings.

4 Experiments

In this section we first outline datasets and implementation details in Sections 4.1 and 4.2. We then validate our implementation of two *state-of the-art* methods for weakly-supervised semantic segmentation in Section 4.3 . Next, we ablate different parameters of the proposed TSEG method for the task of referring expression segmentation in Section 4.4. Finally, we compare TSEG to methods introduced in Section 4.3 on referring expression datasets in Section 4.5.

4.1 Datasets and metrics

Pascal VOC 2012. Pascal [16] is an established benchmark for weakly-supervised semantic segmentation. Following standard practice [1,2,3,33], we augment the original training data with additional images from [22]. The dataset contains 10.5K images for training and 1.5K images for validation.

PhraseCut. PhraseCut [59] is the largest referring expression segmentation dataset with 77K images annotated with 345K referring expressions from Visual Genome [34]. The expressions comprise a wide vocabulary of objects, attributes and relations. The dataset is split into 72K images, 310K expressions for training and 3K images, 14K expressions for validation.

RefCOCO. RefCOCO and RefCOCO+ [65] are the two most commonly used datasets for referring expression segmentation and comprehension. RefCOCO has 20K images and 142K referring expressions for 50K objects while RefCOCO+ contains 20k images and 142K expressions for 50K objects. RefCOCO+ is a harder dataset where words related to the absolute location of the objects are forbidden. RefCOCOg is a dataset of 27K images with 105K expressions referring to 55K objects. Compared to RefCOCO(+), RefCOCOg has longer sentences and richer vocabulary.

Metrics. We follow previous work and report mean Intersection over Union (mIoU) for all Pascal classes. For referring expression segmentation we use standard metrics where mIoU is the IoU averaged over all image-region pairs resulting in a balanced evaluation for small and large objects [65,59].

4.2 Implementation details

Initialization. Our TSEG model contains an image encoder initialized with an ImageNet pre-trained Vision Transformer [15,52] and a text encoder initialized with a pre-trained BERT model [12]. We use ViT-S/16 [52] and BERT-Small [54] which are both expressive models achieving strong performance on vision and language tasks, while remaining fast and compact. Our model has a total number of 42M parameters. Following [15,53], we bilinearly interpolate ViT position embeddings when using an image resolution that differs from its pre-training.

Optimization. For weakly-supervised learning, we use SGD optimizer [50] with a base learning rate γ_0, and set weight decay to 10^{-4}. Following DeepLab [9], we adopt the poly learning rate decay $\gamma = \gamma_0(1 - \frac{n_{iter}}{n_{total}})^{0.9}$. We use a stochastic drop path rate [26] of 0.1 following standard practices to train transformers [12,15,52]. For Pascal, PhraseCut and RefCOCO, we set the base learning rate $\gamma_0 = 10^{-3}$. We found this learning scheme to be stable resulting in good results for all three datasets. Regarding training iterations and the batch size, we use 16K iterations and batches of size 16 for Pascal, 80K iterations and batches of size 32 for RefCOCO, and 120K iterations with batches of size 32 for PhraseCut. When

Method	Image encoder	Class encoding		mIoU
		Vector	Language model	
GAP [2]	WideResNet38	✓	✗	48.0
GAP [2]†	WideResNet38	✗	✓	46.8
GAP [2]†	ViT-S/16	✗	✓	50.2
GMP [68]†	WideResNet38	✗	✓	44.3
GMP [68]†	ViT-S/16	✗	✓	48.1
SPA [3]	WideResNet38	✓	✗	62.7
SPA [3]†	WideResNet38	✗	✓	62.4
SPA [3]†	ViT-S/16	✗	✓	**66.4**

Table 1: State-of-the-art single-stage methods for weakly-supervised semantic segmentation on the Pascal VOC validation set. † denotes our implementation. Multi-scale processing and CRF are used for inference.

training on referring expressions, we randomly sample three positive expressions per image on average. The resolution of images at train time is set to 384×384 and following standard practices we use random rescaling, horizontal flipping and random cropping.

For the fully-supervised setup we use AdamW [32,43] optimizer and set the base learning rate γ_0 to 5×10^{-5}. We set the batch size to 16 for all datasets and use the same number of iterations as for weakly-supervised setups. The resolution of images at train time is 512×512.

4.3 State-of-the-art methods for weakly-supervised semantic segmentation

As we are the first to propose an approach for weakly-supervised learning for referring expression segmentation, we implemented state-of-the-art methods for weakly-supervised semantic segmentation to use as baselines. We use three single-stage methods presented in Section 3.2, namely GMP [68], the seminal work GAP [2], and the more recent state-of-the-art approach SPA [3]. SPA performs close to the best two-stage weakly-supervised methods, DRS [31] and EPS [36], two more complex methods relying on off-the-shelf saliency detectors, which is not the focus of our work.

Table 1 reports the performance on the Pascal VOC 2012 dataset. With a language model as class encoding as shown in Figure 2, we obtain similar performances as GAP [2] and SPA [3] using the same WideResNet38 backbone. By using the more recent ViT-S/16 backbone with SPA, we obtain 66.4% mIoU, a 4% gain over WideResNet38. We also report results with GMP [68] for which we did not find methods reporting results on Pascal VOC 2012. The GMP results are below the GAP results and again the ViT-S/16 backbone gives improved results. In the following sections we use ViT-S/16 as the image encoder, BERT-Small as the text encoder and GAP, GMP and SPA as a point of comparison

$\lambda \downarrow$ $p \rightarrow$	0	1	3	5
0.0	26.8	27.4	27.9	27.7
0.01	26.8	26.8	27.6	**28.3**
0.1	26.3	26.8	27.2	28.0

(a) Size penalty term.

Dimension	mIoU
384	28.3
512	28.6
1024	**28.8**

(b) Multi-modal embedding dimension.

Similarity	mIoU
identity	**28.8**
tf-idf	28.4

(c) Ground truth similarity score.

Dataset Size	mIoU
10%	16.2
50%	25.3
100%	28.8

(d) Dataset size.

Dataset	mIoU
ImageNet	28.8
COCO	**31.7**

(e) Pretraining dataset.

Table 2: Ablations of TSEG with ViT-S/16 as the image encoder and Bert-Small as the language model on PhraseCut validation set.

to our proposed TSEG method. The models can directly be used to perform referring expression segmentation by replacing the class label given as input to the language model by referring expressions.

4.4 TSEG ablations

We now perform weakly-supervised referring expression segmentation. At train time the model has to maximize the score of the image and text embeddings of correct pairings while minimizing the score of incorrect pairings. At test time, following the standard visual grounding setting, the model is given as input the set of referring expressions present in the image and outputs a mask for each referring expression. TSEG uses the proposed MPA to compute scores from patch-text similarities.

Table 2 reports ablations of our TSEG model on the PhraseCut validation set. First, we ablate over the size penalty parameters λ and p from Eq. 7 in Table 2a. Smaller λ values induce a larger penalty for masks with a small size and larger p values increase the focal penalty term, see [39] for more details. We find TSEG is quite robust to the objective hyperparameters λ and p. The best values are $\lambda = 0.01$ and $p = 5$; we fix λ and p to these values in the remaining of the paper. Table 2b reports performance for different cross-modal embedding dimension, increasing the embedding size improves results overall. In Table 2c, we consider different definitions for the ground truth. In the *identity* setup, two referring expressions of a batch are considered the same if they exactly match. In the *tf-idf* setup, the similarity between two referring expressions if computed according to a tf-idf score. If a *tabby cat* is present in an image, and there is a *brown cat* in a second image, the ground truth score for *brown cat* in the first image will be positive because both referring expression share the word *cat*.

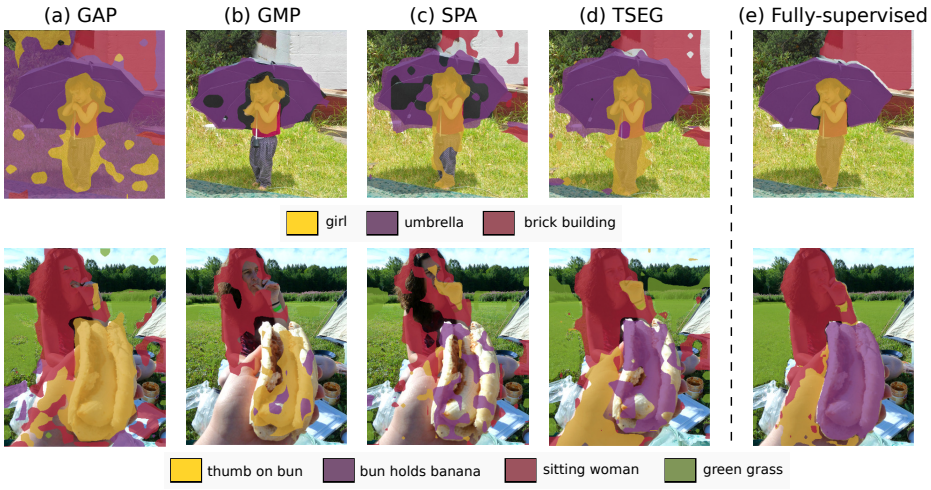

Fig. 4: Comparison of different pooling mechanisms for weakly supervised segmentation from referring expressions on example images from the PhraseCut dataset: (a) Global average pooling (GAP), (b) Global max pooling (GMP), (c) Single-label patch assignment (SPA), (d) TSEG with multi-label patch assignment (TSEG). (e) Fully supervised results.

Using tf-idf performed slightly worse than the identity score and we thus use *identity* to define the ground truth. Table 2d reports the validation score for an increasing training dataset size. We observe that TSEG improves with the dataset size, a desirable property of weakly-supervised segmentation approach where annotations are much cheaper to collect than in the fully-supervised case. Finally, Table 2e reports results when pretraining the visual backbone on only ImageNet for classification or by additionally pretraining the visual and language model on RefCOCO for visual grounding. For pretraining on COCO we use box ground truth annotations as follows. The model is given as input an image and referring expressions to detect, for each referring expressions the model predicts patches that are within the object bounding box. We observe that leveraging detection related information as pretraining improves the result by 3%. In the following we report results with ImageNet pretraining only, following standard practice from the weakly-supervised semantic segmentation literature.

4.5 Weakly supervised referring expression segmentation

We now compare TSEG on referring expression datasets to weakly supervised *state-of-the-art* methods presented in Section 4.3, we report results in Table 3 and show qualitative results in Figure 4.

PhraseCut: GMP and GAP achieve an mIoU of 5.7 and 9.3 respectively, showing that it is possible to learn meaningful masks using referring expressions as labels. However, GAP averages patch-text similarity scores and depends on

Method	PhraseCut	RefCOCO	RefCOCO+	RefCOCOg
GMP [68]†	5.77	6.54	5.12	6.54
GAP [2]†	9.35	6.65	7.21	6.07
SPA [3]†	21.12	10.32	9.16	8.35
TSEG	28.77	25.44	22.01	22.05
TSEG (CRF)	**30.12**	**25.95**	**22.62**	**23.41**

Table 3: Comparison of different weakly-supervised methods for referring expression segmentation on Phrasecut and RefCOCO validation set. † denotes our implementation, validated in Table 1.

Fig. 5: TSEG segmentation results on the PhraseCut test set. Our method segments a rich set of open-vocabulary concepts without using pixel-level supervision at the training.

the instance mask size which tends to generate over-saturated activation maps (Fig. 4a). GMP exhibits complementary properties focusing on the most discriminative object parts (Fig. 4b). SPA outperforms GAP and GMP with a mIoU of 21.1, consistent with results on Pascal VOC 2012, see Table 1. MPA further improves SPA by 7%, with 28.77% mIoU on Phrasecut, showing its crucial importance for referring expression segmentation. This improvement can partly be explained by the fact that our objective allows multiple masks to overlap by design, a highly desirable property that is not satisfied by GMP, GAP and SPA. From Figure 4d we observe that MPA generates more complete masks with both higher recall, e.g. the *thumb on bun* instance is detected, and we obtain higher precision, e.g. masks achieve better completeness as for the *sitting woman* instance. Using CRF [8] further improves the performance to 30.12 mIoU. Qualitative results are presented in Figure 5.

To obtain an upper-bound, we also train TSEG with full supervision and obtain a 49.6 mIoU. This is close to the best fully supervised method MDETR [29], which obtains 53.1 mIoU while pretraining on a much large dataset annotated for visual grounding and higher training resolution. While there is still a gap compared to full supervision, we believe our proposed results to be promising and the first step towards large-scale weakly supervised referring expression segmentation. Additional qualitative results and comparison to the fully-supervised

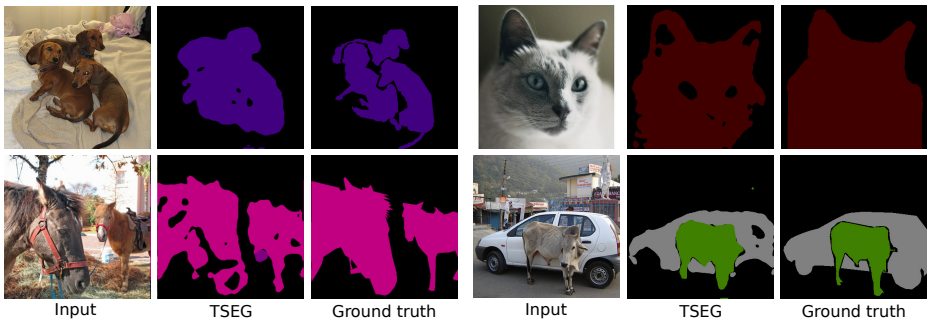

Fig. 6: Zero-shot transfer of our approach TSEG trained from text supervision on PhraseCut and evaluated on Pascal VOC 2012. The method has not been explicitly trained for PASCAL classes and has never obtained pixel-level supervision.

model are presented in the appendix.

RefCOCO: We also evaluate our method on the three RefCOCO datasets and report results on the *val* split in Table 3. Again, MPA outperforms GMP, GAP and SPA by a large margin. Training TSEG with full supervision we obtain 66.00 mIoU on RefCOCO, 55.35 on RefCOCO+ and 54.71 on RefCOCOg. This is slightly better than the best fully supervised method VLT [13], which obtains 65.65, 55.50 and 52.99 mIoU respectively. There is a larger gain from using full supervision than on PhraseCut. This could be explained by more fine-grained referring expressions such as *broccoli stalk that is pointing up and is touching a sliced carrot* or *a darker brown teddy bear in a row of lighter teddy bears* that are harder to localize without pixel-level supervision.

4.6 Zero-shot transfer on Pascal VOC

We evaluate the ability of TSEG to detect and localize visual concepts from text supervision by performing zero-shot experiments on Pascal VOC 2012 dataset, see Fig. 6. We take our TSEG model trained on the PhraseCut dataset, i.e., with the text supervision based on the referring expressions from PhraseCut. We, then, pass the names of Pascal classes as input to the text encoder and obtain segmentation masks and confidence scores for all 20 object classes in each image. We filter classes by thresholding with the model confidence scores then use argmax between the remaining masks to determine the class of each pixel. We set the threshold to 0.5.

In the zero-shot setting, our TSEG model achieves an mIoU of 48.5 while the SPA baseline achieves an mIoU of 43.5. Interestingly, TSEG performs well on all classes except the *person* class. As can be observed from Figure 7, the model does not detect the *person* label, but can be improved with label engineering by using more specific labels for the text encoder, such as *woman* and *rider*.

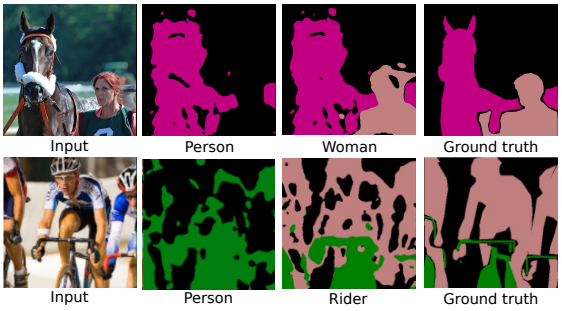

Fig. 7: Failure cases on the person class for zero-shot results on Pascal VOC 2012. While the horse (violet) or bicycle (green) are well localized, the class person (pink) is not detected with the *person* label (column 2). The model detects it by using more specific labels such as *rider* or *woman* (column 3, pink). Column 4 shows the ground truth.

This bias partly comes from the annotations of PhraseCut training set and we believe that the need for label engineering may be reduced by training TSEG on a larger dataset with richer text annotations. On the person class, by passing *person* as input to the text encoder we obtain an IoU of 0.6 while by merging masks for the words *man, woman, men, women, child, boy, girl, baby* we improve the IoU to 30.4. By performing label engineering, TSEG reaches 50.3 mIoU. In comparison, GroupViT [61] reports an mIoU of 51.2, but it has been trained on a much larger dataset of 30M image-text pairs and was designed for zero-shot segmentation. TSEG performs comparably to GroupViT, while trained on 350k image-text pairs. This demonstrates the ability of our approach to learn general visual concepts accurately.

5 Acknowledgements

This work was partially supported by the HPC resources from GENCI-IDRIS (Grant 2021-AD011011163R1), the Louis Vuitton ENS Chair on Artificial Intelligence, and the French government under management of Agence Nationale de la Recherche as part of the "Investissements d'avenir" program, reference ANR-19-P3IA-0001 (PRAIRIE 3IA Institute).

6 Conclusion

This work introduces TSEG for weakly-supervised referring expression segmentation. We propose a multi-label patch assignment (MPA) mechanism that improves previous methods by a margin on this task. We believe our work makes an important step towards scalable image segmentation from natural language. Future work will address how to reduce the performance gap between weakly supervised and fully supervised methods and segment regions directly from image captions.

References

1. Ahn, J., Cho, S., Kwak, S.: Weakly supervised learning of instance segmentation with inter-pixel relations. In: CVPR (2019)
2. Ahn, J., Kwak, S.: Learning pixel-level semantic affinity with image-level supervision for weakly supervised semantic segmentation. In: CVPR (2018)
3. Araslanov, N., Roth, S.: Single-stage semantic segmentation from image labels. In: CVPR (2020)
4. Arnab, A., Dehghani, M., Heigold, G., Sun, C., Lucic, M., Schmid, C.: ViViT: A video vision transformer. ICCV (2021)
5. Bilen, H., Pedersoli, M., Tuytelaars, T.: Weakly supervised object detection with posterior regularization. In: BMVC (2014)
6. Bojanowski, P., Lajugie, R., Bach, F., Laptev, I., Ponce, J., Schmid, C., Sivic, J.: Weakly supervised action labeling in videos under ordering constraints. In: ECCV (2014)
7. Chen, K., Gao, J., Nevatia, R.: Knowledge aided consistency for weakly supervised phrase grounding. In: CVPR (2018)
8. Chen, L., Papandreou, G., Kokkinos, I., Murphy, K., Yuille, A.L.: Deeplab: Semantic image segmentation with deep convolutional nets, atrous convolution, and fully connected crfs. IEEE Trans. Pattern Anal. Mach. Intell. **40**(4), 834–848 (2018)
9. Chen, L., Zhu, Y., Papandreou, G., Schroff, F., Adam, H.: Encoder-decoder with atrous separable convolution for semantic image segmentation. In: ECCV (2018)
10. Chen, T., Kornblith, S., Norouzi, M., Hinton, G.E.: A simple framework for contrastive learning of visual representations. In: ICML (2020)
11. Cheng, B., Schwing, A.G., Kirillov, A.: Per-pixel classification is not all you need for semantic segmentation. In: NIPS (2021)
12. Devlin, J., Chang, M., Lee, K., Toutanova, K.: BERT: pre-training of deep bidirectional transformers for language understanding. In: NAACL-HLT (2019)
13. Ding, H., Liu, C., Wang, S., Jiang, X.: Vision-language transformer and query generation for referring segmentation. In: ICCV (2021)
14. Doersch, C., Gupta, A., Efros, A.A.: Unsupervised visual representation learning by context prediction. In: ICCV (2015)
15. Dosovitskiy, A., Beyer, L., Kolesnikov, A., Weissenborn, D., Zhai, X., Unterthiner, T., Dehghani, M., Minderer, M., Heigold, G., Gelly, S., Uszkoreit, J., Houlsby, N.: An image is worth 16x16 words: Transformers for image recognition at scale. In: ICLR (2021)
16. Everingham, M., Gool, L.V., Williams, C.K.I., Winn, J.M., Zisserman, A.: The pascal visual object classes (VOC) challenge. IJCV **88**(2), 303–338 (2010)
17. Fan, R., Cheng, M., Hou, Q., Mu, T., Wang, J., Hu, S.: S4Net: Single stage salient-instance segmentation. In: CVPR (2019)
18. Fan, R., Hou, Q., Cheng, M., Yu, G., Martin, R.R., Hu, S.: Associating inter-image salient instances for weakly supervised semantic segmentation. In: ECCV (2018)
19. Ghadiyaram, D., Tran, D., Mahajan, D.: Large-scale weakly-supervised pre-training for video action recognition. In: CVPR (2019)
20. Ghiasi, G., Gu, X., Cui, Y., Lin, T.: Open-vocabulary image segmentation. CoRR (2021)
21. Gupta, T., Vahdat, A., Chechik, G., Yang, X., Kautz, J., Hoiem, D.: Contrastive learning for weakly supervised phrase grounding. In: ECCV (2020)
22. Hariharan, B., Arbelaez, P., Bourdev, L.D., Maji, S., Malik, J.: Semantic contours from inverse detectors. In: ICCV (2011)

23. He, K., Gkioxari, G., Dollár, P., Girshick, R.B.: Mask R-CNN. In: ICCV (2017)
24. Hu, R., Rohrbach, M., Darrell, T.: Segmentation from natural language expressions. In: ECCV (2016)
25. Hu, Z., Feng, G., Sun, J., Zhang, L., Lu, H.: Bi-directional relationship inferring network for referring image segmentation. In: CVPR (2020)
26. Huang, G., Sun, Y., Liu, Z., Sedra, D., Weinberger, K.Q.: Deep networks with stochastic depth. In: ECCV (2016)
27. Huang, Z., Wang, X., Wang, J., Liu, W., Wang, J.: Weakly-supervised semantic segmentation network with deep seeded region growing. In: CVPR (2018)
28. Jia, C., Yang, Y., Xia, Y., Chen, Y., Parekh, Z., Pham, H., Le, Q.V., Sung, Y., Li, Z., Duerig, T.: Scaling up visual and vision-language representation learning with noisy text supervision. In: ICML (2021)
29. Kamath, A., Singh, M., LeCun, Y., Misra, I., Synnaeve, G., Carion, N.: MDETR - modulated detection for end-to-end multi-modal understanding. ICCV (2021)
30. Kantorov, V., Oquab, M., Cho, M., Laptev, I.: Contextlocnet: Context-aware deep network models for weakly supervised localization. In: ECCV (2016)
31. Kim, B., Han, S., Kim, J.: Discriminative region suppression for weakly-supervised semantic segmentation. In: AAAI (2021)
32. Kingma, D.P., Ba, J.: Adam: A method for stochastic optimization. In: ICLR (2015)
33. Kolesnikov, A., Lampert, C.H.: Seed, expand and constrain: Three principles for weakly-supervised image segmentation. In: ECCV (2016)
34. Krishna, R., Zhu, Y., Groth, O., Johnson, J., Hata, K., Kravitz, J., Chen, S., Kalantidis, Y., Li, L., Shamma, D.A., Bernstein, M.S., Fei-Fei, L.: Visual genome: Connecting language and vision using crowdsourced dense image annotations. IJCV **123**(1), 32–73 (2017)
35. Lee, J., Kim, E., Lee, S., Lee, J., Yoon, S.: Frame-to-frame aggregation of active regions in web videos for weakly supervised semantic segmentation. In: ICCV (2019)
36. Lee, S., Lee, M., Lee, J., Shim, H.: Railroad is not a train: Saliency as pseudo-pixel supervision for weakly supervised semantic segmentation. In: CVPR (2021)
37. Li, D., Huang, J.B., Li, Y., Wang, S., Yang, M.H.: Weakly supervised object localization with progressive domain adaptation. In: CVPR (2016)
38. Li, L.H., Yatskar, M., Yin, D., Hsieh, C., Chang, K.: VisualBERT: A simple and performant baseline for vision and language. arXiv preprint arXiv:1908.03557 (2019)
39. Lin, T., Goyal, P., Girshick, R.B., He, K., Dollár, P.: Focal loss for dense object detection. IEEE Trans. Pattern Anal. Mach. Intell. **42**(2), 318–327 (2020)
40. Liu, X., Li, L., Wang, S., Zha, Z., Meng, D., Huang, Q.: Adaptive reconstruction network for weakly supervised referring expression grounding. In: ICCV (2019)
41. Liu, Y., Wan, B., Ma, L., He, X.: Relation-aware instance refinement for weakly supervised visual grounding. In: CVPR (2021)
42. Liu, Z., Lin, Y., Cao, Y., Hu, H., Wei, Y., Zhang, Z., Lin, S., Guo, B.: Swin transformer: Hierarchical vision transformer using shifted windows. In: ICCV (2021)
43. Loshchilov, I., Hutter, F.: Decoupled weight decay regularization. In: ICLR (2019)
44. Miech, A., Alayrac, J.B., Smaira, L., Laptev, I., Sivic, J., Zisserman, A.: End-to-end learning of visual representations from uncurated instructional videos. In: CVPR (2020)
45. Papandreou, G., Chen, L., Murphy, K.P., Yuille, A.L.: Weakly-and semi-supervised learning of a deep convolutional network for semantic image segmentation. In: ICCV (2015)

46. Pinheiro, P.H.O., Collobert, R.: From image-level to pixel-level labeling with convolutional networks. In: CVPR (2015)
47. Radford, A., Kim, J.W., Hallacy, C., Ramesh, A., Goh, G., Agarwal, S., Sastry, G., Askell, A., Mishkin, P., Clark, J., Krueger, G., Sutskever, I.: Learning transferable visual models from natural language supervision. In: ICML (2021)
48. Ramesh, A., Pavlov, M., Goh, G., Gray, S., Voss, C., Radford, A., Chen, M., Sutskever, I.: Zero-shot text-to-image generation. In: ICML (2021)
49. Ren, S., He, K., Girshick, R.B., Sun, J.: Faster R-CNN: towards real-time object detection with region proposal networks. PAMI **39**(6), 1137–1149 (2017)
50. Robbins, H., Monro, S.: A stochastic approximation method. Annals of Mathematical Statistics (1951)
51. Sennrich, R., Haddow, B., Birch, A.: Neural machine translation of rare words with subword units. In: ACL (2016)
52. Steiner, A., Kolesnikov, A., Zhai, X., Wightman, R., Uszkoreit, J., Beyer, L.: How to train your ViT? data, augmentation, and regularization in vision transformers. arXiv preprint arXiv:2106.10270 (2021)
53. Strudel, R., Pinel, R.G., Laptev, I., Schmid, C.: Segmenter: Transformer for semantic segmentation. ICCV (2021)
54. Turc, I., Chang, M., Lee, K., Toutanova, K.: Well-read students learn better: The impact of student initialization on knowledge distillation. arXiv preprint arXiv:1908.08962 (2019)
55. Vaswani, A., Shazeer, N., Parmar, N., Uszkoreit, J., Jones, L., Gomez, A.N., Kaiser, L., Polosukhin, I.: Attention is all you need. In: NIPS (2017)
56. Wang, J., Jiang, H., Yuan, Z., Cheng, M., Hu, X., Zheng, N.: Salient object detection: A discriminative regional feature integration approach. IJCV **123**(2), 251–268 (2017)
57. Wei, Y., Feng, J., Liang, X., Cheng, M., Zhao, Y., Yan, S.: Object region mining with adversarial erasing: A simple classification to semantic segmentation approach. In: CVPR (2017)
58. Wei, Y., Xiao, H., Shi, H., Jie, Z., Feng, J., Huang, T.S.: Revisiting dilated convolution: A simple approach for weakly- and semi-supervised semantic segmentation. In: CVPR (2018)
59. Wu, C., Lin, Z., Cohen, S., Bui, T., Maji, S.: Phrasecut: Language-based image segmentation in the wild. In: CVPR (2020)
60. Xiao, F., Sigal, L., Lee, Y.J.: Weakly-supervised visual grounding of phrases with linguistic structures. In: CVPR (2017)
61. Xu, J., Mello, S.D., Liu, S., Byeon, W., Breuel, T.M., Kautz, J., Wang, X.: Groupvit: Semantic segmentation emerges from text supervision. CoRR (2022)
62. Xu, M., Zhang, Z., Wei, F., Lin, Y., Cao, Y., Hu, H., Bai, X.: A simple baseline for zero-shot semantic segmentation with pre-trained vision-language model. CoRR (2021)
63. Ye, L., Rochan, M., Liu, Z., Wang, Y.: Cross-modal self-attention network for referring image segmentation. In: CVPR (2019)
64. Yu, L., Lin, Z., Shen, X., Yang, J., Lu, X., Bansal, M., Berg, T.L.: Mattnet: Modular attention network for referring expression comprehension. In: CVPR (2018)
65. Yu, L., Poirson, P., Yang, S., Berg, A.C., Berg, T.L.: Modeling context in referring expressions. In: ECCV (2016)
66. Yu, Z., Zhuge, Y., Lu, H., Zhang, L.: Joint learning of saliency detection and weakly supervised semantic segmentation. In: ICCV (2019)
67. Zabari, N., Hoshen, Y.: Semantic segmentation in-the-wild without seeing any segmentation examples. CoRR (2021)

68. Zhou, B., Khosla, A., Lapedriza, À., Oliva, A., Torralba, A.: Learning deep features for discriminative localization. In: CVPR (2016)
69. Zhou, C., Loy, C.C., Dai, B.: Denseclip: Extract free dense labels from CLIP. CoRR (2021)

7 Appendix

Qualitative results. We present additional qualitative results in Figures 8 and 9. In particular, we compare TSEG trained with weak supervision to the same model trained with full supervision in Figure 8. TSEG captures cloth related concepts, animals and parts of the bodies reasonably well, however it can fail at capturing colors, distinguish between a book and a laptop, or between a blue jean and different type of trousers. In Figure 9, we observe that TSEG captures a rich variety of visual concepts, even rarely occurring ones quite accurately.

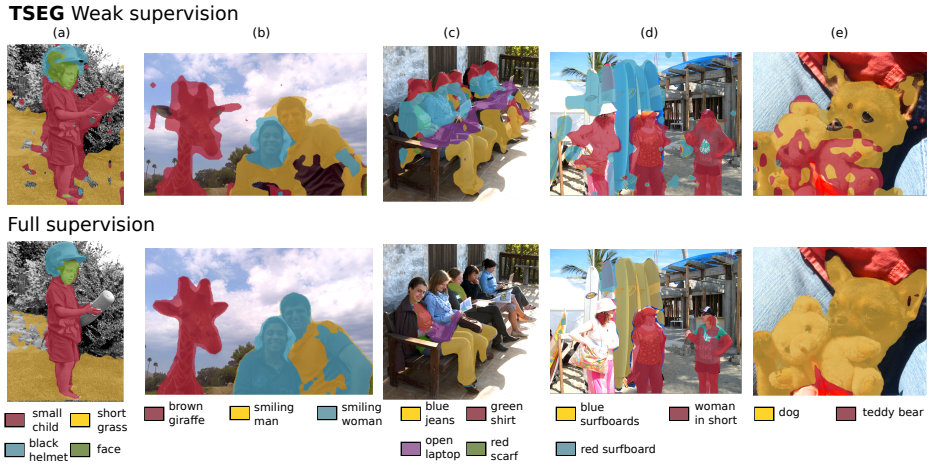

Fig. 8: Comparison of TSEG to fully-supervised results on PhraseCut validation set. (a) Both methods perform well. (b) Both approaches do not distinguish well man and woman. (c-d) TSEG captures coarse semantic meaning such as legs (c) or surfboards (d) but misses the difference between a book and a laptop (c) or color attributes (d). (e) TSEG distinguishes the teddy bear and dog better than the fully-supervised model.

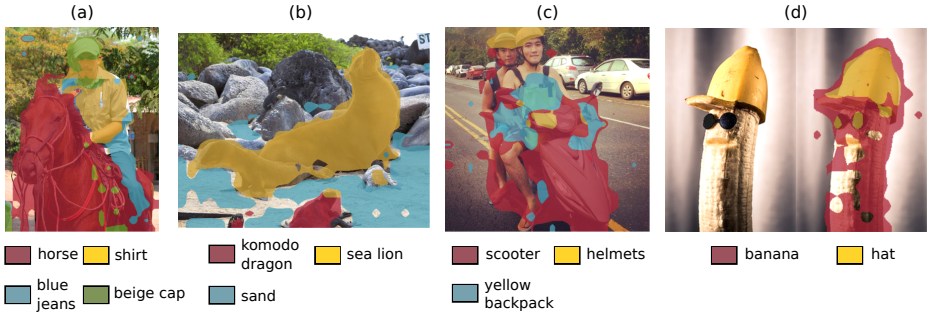

Fig. 9: Additional qualitative results of our approach TSEG. Our approach captures rarely occurring visual concepts such as a komodo dragon or a banana-made hat.